Research Article

BIOMEDICAL Journal of Scientific & Technical Research

ISSN: 2574 -1241

DOI: 10.26717/BJSTR.2020.24.004054

Supplementary Methods for Quantification of Entire Tumor Vascular Normalization in Response to A VEGF Inhibitor

Chung Wein Lee, Jian Wang, Li Li, Todd Christopher, Shuyu Li, Eric Su, Yufeng Lu, Chandrasekar Iyer, Kuldeep Neote, Jeffrey Wolos, Michael Westmore

3-D Vessel Length Distribution

Vessels were defined as being from the root of a vascular tree to the end nodes (Supplementary Figure 1). The vessel length algorithm traced the lengths of all vessels from the shared root to all end nodes of a vascular network. The number of vessels of a vascular tree is identical to the number of end nodes. In the Supplementary Figure 1 cartoon example, there were six vessels in the vascular tree. The length measurement was converted from a voxel number to millimetres by multiplying by 0.016mm. The algorithm was applied to all images. The vessel length histograms in the same group were binned together and then normalized by the total number of vessels.

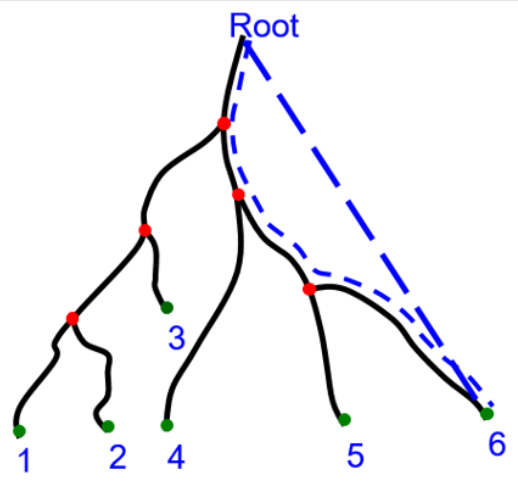

Supplementary Figure 1: Vasculature cartoon to illustrate the definitions of the imaging markers.
Green circles represent the end nodes of the vascular tree; red circles represent the branch points of the vascular tree. A vessel of the vascular tree extends from the root of the tree to one of the end nodes. Accordingly, the number of end nodes is equal to the number of vessels. A total of six vessels are counted in this 2-D vasculature demonstration. Tortuosity is defined as the true length of the vessel divided by the shortest length between the ends of the vessel. In the example of Vessel 6, the tortuosity is equal to the length ratio of the short-dashed line to the long-dashed line. Vessel segments are between two branch points (red dots) or between a branch point and an end point (green dot).

3-D Vessel Tortuosity Distribution

The tortuosity definition of a single vessel is the ratio of the true length of the vessel to the shortest distance between the ends of the vessel (Supplementary Figure 1, Vessel 6 demonstration). The 3-D tortuosity algorithm calculated the tortuosity value of all the vessels from a vascular tree. The vessels with tortuosity equal to one and two were ignored. The tortuosity histograms from the same group were binned together and normalized by the total number of vessels. The vessels were further grouped into three domains: low tortuosity vessels (tortuosity from 3 to 12), high tortuosity vessels (tortuosity from 13 to 70), and ultrahigh tortuosity vessels (tortuosity above 70).

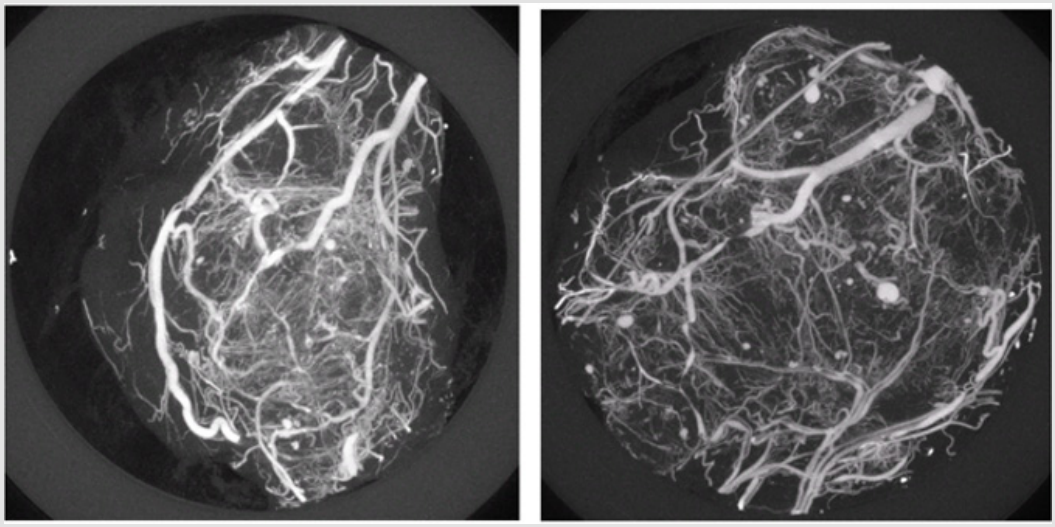

Supplementary Figure 2: Identical vessel branch point fractal dimensions of two tumor vascular networks. Two vasculature maximum intensity projection images of two-week vehicle mice are shown in this example. Two female CB-17 SCID mice were implanted with the same number of A549 cells and were housed under identical growth conditions. Clear vascular morphological distinctions, such as branch point locations and vessel density, between the two vascular structures are demonstrated. The fractal dimension, D0, from the 3-D branch point locations of vascular tree A was 2.336; the branch point fractal dimension of vascular tree B was 2.332.

Vascular Volume Estimation

The vascular volume algorithm counted the total number of voxels of the vascular structure within the threshold. The vascular volume in voxel numbers was converted to mm^3 by multiplying by the physical dimensions of a voxel $(0.016\ mm)^3$. One-way ANOVA was applied to evaluate the significance of the average vascular volume differences between vehicle and related Sutent-treated groups.

Micro-Vessel Segment Lumen Surface Area

The cross-sectional area algorithm applied a sample disk to count the number of pixels perpendicular to the local vessel axis of a vascular tree. The number of selected pixels represented the cross-sectional area. The cross-sectional area in units of mm^2 was derived by multiplying by the physical area of a pixel $(0.016\ mm)^2$. We used the circular area formula (πR^2) to derive the circumference. The product of circumference and slice thickness represents the surface area. To calculate the precise surface area of micro-vessel segments, we adopted small sample disks with radii 2,3, and 4 pixels to evaluate precisely the surface area contribution from segments with diameters less than 50,70, and 107 μ m, respectively.

A segment from a vessel was defined as the part of the vessel between two branch points or between a branch point and an end node. The algorithm excluded vessel segments with lengths less than four pixels. Only segments with average diameters less than the required threshold were selected. The cross-sectional area and surface area algorithms were then applied. The total surface area was the summation of the surface area contributions from all eligible vessel segments. For the micro-vessel surface area from segments with diameters less than thresholds of 70 and 107 μ m, the same algorithm was performed with sample disks of radii three and four.

Vessel Segment Diameter Distribution of Vehicle Groups

Similarly, to the micro-vessel surface area algorithm, the vessel segment diameter was derived from the vessel segment cross-sectional area. A sample disk with a radius of 20 pixels was applied to acquire the cross-sectional area. The average diameter of the vessel segment was derived from the cross-sectional area via the circular area formula (πR^2). The maximum diameter based upon the sample disk radius of 20 pixels was approximately 0.67 mm. The vessel segment diameter histograms of the one-week and two-week vehicle groups were summed and then normalized by the total segment number of the group.

Generalized Fractal Dimension Based Upon Branch Point Locations

Fractal dimension analysis has been adapted to characterize the local and global vascular networks (Agaimy et al., 2007; Baish and Jain, 2000; Gazit et al., 1997; Zamir, 2001) and to reveal the normalization due to anti-angiogenic therapies(Jain, 2003).

Fractal analysis has been applied in other scientific fields to illustrate the different components of intrinsic nonlinear properties(Agaimy et al., 2007; Kurths and Herzel, 1987; Wang and Lee, 1995). Branch points signify blood flow division to more than one direction. The location of branch points might be related to the nutrient distribution and delivery efficiency in an organ. Based upon the above rationale we calculated the generalized fractal dimensions

from the locations of branch points in a vascular structure. The generalized fractal dimension algorithm can be found in references (Grassberger, 1983; Hentschel and Procaccia, 1983; Wang and Lee, 1996). Here we only report the fractal dimension associated with q=0(Hentschel and Procaccia, 1983).

References

1. Agaimy A (2007) Minute gastric sclerosing stromal tumors (GIST tumorlets) are common in adults and frequently show c-KIT mutations. Am J Surg Pathol 31(1):113-120.
2. Alitalo K (2005) Lymphangiogenesis in development and human disease. Nature 438(7070): 946-953.
3. Baish JW, Jain RK (2000) Fractals and cancer. Cancer Res 60(14): 3683-3688.
4. Bostwick DG (2000) Prognostic factors in prostate cancer. College of American Pathologists Consensus Statement 1999. Archives of Pathology & Laboratory Medicine 124(7): 995-1000.
5. Cabebe E,Wakelee H (2006) Sunitinib: a newly approved small-molecule inhibitor of angiogenesis. Drugs Today (Barc) 42(6): 387-398.
6. Carmeliet P (2003) Angiogenesis in health and disease. Nat Med 9(6): 653-660.
7. Carmeliet P (2005) Angiogenesis in life, disease and medicine. Nature. 438(7070): 932-936.
8. Carmeliet P, Jain RK (2000) Angiogenesis in cancer and other diseases. Nature 407(6801): 249-257.
9. Carmeliet P, Tessier Lavigne M (2005) Common mechanisms of nerve and blood vessel wiring. Nature 436 193-200.
10. Demetri GD (2006) Efficacy and safety of sunitinib in patients with advanced gastrointestinal stromal tumour after failure of imatinib: a randomised controlled trial. Lancet 368(9544): 1329-1338.
11. Faivre S (2006) Safety, pharmacokinetic, and antitumor activity of SU11248, a novel oral multitarget tyrosine kinase inhibitor, in patients with cancer. J Clin Oncol 24(1): 25-35.
12. Faivre S (2007) Molecular basis for sunitinib efficacy and future clinical development. Nat Rev Drug Discov 6(9): 734-45.
13. Ferrara N (2003) The biology of VEGF and its receptors. Nat Med 9(6): 669-676.
14. Folkman J (1971) Tumor angiogenesis: therapeutic implications. New England Journal of Medicine. 285(21): 1182-1186.
15. Folkman J (1990) What Is the Evidence That Tumors Are Angiogenesis Dependent? J Natl Cancer Inst 82(1): 4-7.
16. Folkman J (2007) Angiogenesis: an organizing principle for drug discovery? Nat Rev Drug Discov 6(4): 273-286.
17. Gazit Y (1997) Fractal characteristics of tumor vascular architecture during tumor growth and regression. Microcirculation 4(4): 395-402.
18. Grassberger P (1983) Generalized Dimensions of Strange Attractors. Phyiscs Letters. 97(6) 227-230.
19. Greenberg DA, Jin K (2005) From angiogenesis to neuropathology. Nature 438(7070): 954-959.
20. Hashizume H (2000) Openings between Defective Endothelial Cells Explain Tumor Vessel Leakiness. Am J Pathol 156(4): 1363-1380.
21. Hentschel HE, Procaccia I (1983) The Infinite Number of Generalized Dimensions of Fractals and Strange Attractors. Physica D 8(3): 435-444.
22. Hicklin DJ, Ellis LM (2005) Role of the vascular endothelial growth factor pathway in tumor growth and angiogenesis. J Clin Oncol 23(5): 1011-1027.
23. Hlatky L (2002) Clinical Application of Antiangiogenic Therapy: Micro vessel Density, What It Does and Doesn't Tell Us. J Natl Cancer Inst 94(12): 883-893.
24. Jain RK (2001) Normalizing tumor vasculature with anti-angiogenic therapy: a new paradigm for combination therapy. Nat Med 7(9): 987-989.
25. Jain RK (2003) Molecular regulation of vessel maturation. Nat Med 9(6): 685-693.
26. Jain RK (2005a) Antiangiogenic therapy for cancer: current and emerging concepts. Oncology (Williston Park). 19: 7-16.
27. Jain RK (2005b) Normalization of tumor vasculature: an emerging concept in antiangiogenic therapy. Science 307(5706): 58-62.
28. Jain RK (2006) Lessons from phase III clinical trials on anti-VEGF therapy for cancer. Nat Clin Pract Oncol. 3(1): 24-40.
29. Kurths J, Herzel H (1987) An Attractor in a Solar Time Series. Physica D 25(1-3): 165-172.
30. May NA (2002) Method and timing of tumor volume measurement for outcome prediction in cervical cancer using magnetic resonance imaging. International Journal of Radiation Oncology Biology Physics 52(1): 14-22.
31. McDonald DM, Choyke PL (2003) Imaging of angiogenesis: from microscope to clinic. Nat Med 9(6): 713-725.
32. Miller TR, Grigsby PW (2002) Measurement of tumor volume by PET to evaluate prognosis in patients with advanced cervical cancer treated by radiation therapy. International Journal of Radiation Oncology Biology Physics. 53(2): 353-359.
33. Motzer RJ (2006a) Activity of SU11248, a Multitargeted Inhibitor of Vascular Endothelial Growth Factor Receptor and Platelet-Derived Growth Factor Receptor, in Patients with Metastatic Renal Cell Carcinoma. J Clin Oncol 24(1): 16-24.
34. Motzer RJ (2006b) Sunitinib in Patients with Metastatic Renal Cell Carcinoma. JAMA 295(21): 2516-2524.
35. Nagy JA (2002) VEGF-A induces angiogenesis, arteriogenesis, lymphangiogenesis, and vascular malformations. Cold Spring Harb Symp Quant Biol 67: 227-237.
36. Richardson TP (2001) Polymeric system for dual growth factor delivery. Nat Biotechnol 19(11): 1029-1034.
37. Sakamoto KM (2004) Su-11248 Sugen. Curr Opin Investig Drugs 5(12): 1329-1339.
38. Teicher BA (1996) A systems approach to cancer therapy. (Antioncogenics + standard cytotoxics-->mechanism(s) of interaction). Cancer Metastasis Rev. 15(2): 247-272.
39. Wan SY (2002) Multi-generational analysis and visualization of the vascular tree in 3D micro-CT images. Comput Biol Med 32(2): 55-71.
40. Wang J, Lee C (1995) Fractal characterization of an earthquake sequence. Physica A 221(1-3): 152-158.
41. Wang J, Lee C (1996) Multifractal Measures of Earthquakes in West Taiwan. PURE APPL GEOPHYS. 146: 131-145.
42. Watanabe H (2003) Tumor response to chemotherapy: The validity and reproducibility of RECIST guidelines in NSCLC patients. Cancer Science. 94(11): 1015-1020.
43. Zamir M (2001) Fractal dimensions and multifractality in vascular branching. J Theor Biol 212(2): 183-190.